

# Modeling and Optimization of Variability in High-k/Metal-Gate MOSFETs

T-H Yu, Tetsu Ohtou, K-M Liu\*, W-Y Chen, Y-P Hu, C-F Cheng, and Y-M Sheu

Taiwan Semiconductor Manufacturing Company (TSMC), R&D

\*National Nano Device Laboratory (NDL)

Hsinchu, Taiwan R.O.C.

e-mail: thyub@tsmc.com

**Abstract**—We present an in-house tool to simulate random dopant fluctuation effects on nano-scale devices with non-uniform channel doping profiles. A novel dopant discretization scheme using Poisson statistics that can achieve self-consistent median parametric values (e.g. average channel concentration) with deterministic device simulations was introduced. This capability was deployed to study the variability contributed from random dopant fluctuation and critical dimension uniformity under different work function shift in advanced transistor structures with non-uniform channels. It is concluded that work function shift can be employed to minimize the total variability.

**Keywords**—random dopant fluctuation; variability; high-k/metal gate

## I. INTRODUCTION

High-K metal-gate (HKMG) process has been introduced into sub-45nm MOSFETs because it can scale down the effective oxide thickness (EOT) without raising the gate leakage current. Hence, work function shift (WFS) in HKMG devices becomes a parameter that needs to be optimized according to performance and  $V_{th}$  variation [1]. It is also recognized that random dopant fluctuation (RDF) is considered a key contributor to  $V_{th}$  variation [2]. Furthermore, most prior works on RDF numerical studies relied on uniform channel assumption [3][4] which is not consistent with advanced transistor design. In this paper, we propose a unique atomistic simulation methodology to predict RDF. In our methodology, a new dopant discretization scheme has been implemented into the simulator which can take non-uniform doping profiles into account. We also demonstrate that the variability due to RDF and  $V_{th}$  variation induced by critical dimension uniformity (CDU) can be minimized through the WFS optimization.

## II. TRANSISTOR DESIGN

The initial simulation templates have been well calibrated with silicon [5], including junction profiles and electrical characteristics. After that, further optimization to achieve the best performance consists of ultra shallow junction, spacer, pocket/LDD, and S/D optimization.

## III. MODELLING OF RDF

Fig. 1 shows the simulation flow for RDF. It starts from a TIF file generated from a well calibrated TSUPREM-4

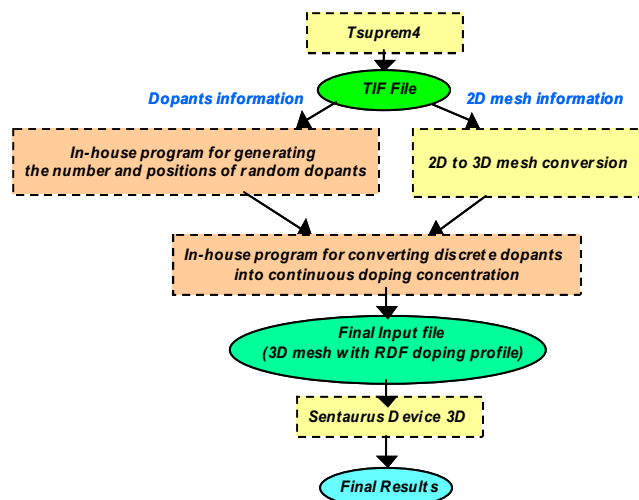


Figure 1. In-house simulation flow for RDF.

template. Basically, the program deals with two major components, grid points and doping concentration, in the simulation. For grid points, 2D mesh is extended to 3D to prepare the following 3D device simulation. For doping concentration, the continuous doping distribution from TS4 has to be converted to discrete dopants by Poisson statistical distribution. To incorporate into 3D device simulator, the discrete dopants are further converted to continuous dopant distribution followed by a long-range coulomb potential calculation. Therefore, the 3D RDF effect on device characteristics can be obtained.

Based on the information of mesh and dopant concentration contained in the TIF file, for each grid point we can generate the corresponding discrete random dopants whose number is determined by Poisson statistics (the mean of Poisson distribution is equal to dopant concentration multiplied by mesh volume) using Monte Carlo (MC) method and locations are distributed randomly within the mesh. The coulomb potential of discrete ionized dopants can be separated into two different components, long-range and short-range parts because ionized impurity exhibits both collective and individual potential behaviors. A long-range coulomb interaction arises from the collective oscillation of the ionized impurity while

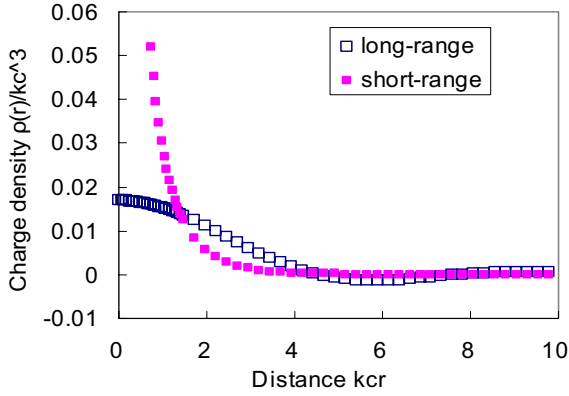


Figure 2. charge density of a single dopant for long-range shown in eq.2 and short-range as a function of distance

ionized impurity on shorter scale behaves more as a collective of individual charge particle [6]. In this simulation we only take the long-range part into account for two reasons. First, the discrete dopant including long and short range parts becomes divergent at the origin. Second, the electric potential obtained from Poisson solver in DD (Drift-Diffusion) simulator represents the long-range part of coulomb potential [7]. Therefore to avoid a singularity in the potential profile and incorporate into 3D DD simulation, the long-range part is utilized to construct an atomic potential distribution. The discrete dopant potential can be derived from the Fourier transformation of ionized impurity potential in k-space [8]. The long-range and short-range parts are separated by the integration ranges with  $|k| < kc$  and  $|k| > kc$ , where  $kc$  is the inverse of the screening length.

$$k_c = \sqrt{\frac{q^2 N_A}{\epsilon k_b T}}, \quad (1)$$

where  $\epsilon$  is the dielectric constant and  $N_A$  is the acceptor doping concentration for p-type substrate.

Then the charge density is solved from the Poisson equation. The long-range and short-range charge density generated from a single dopant is shown in Fig. 2. As can be

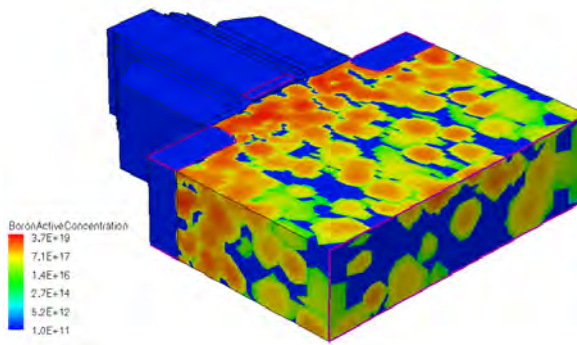


Figure 3. The boron doping profile after considering RDF for further SDevice 3D simulation

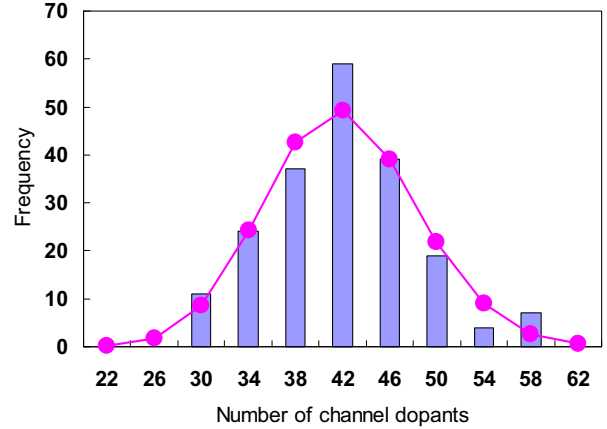


Figure 4. The distribution of the number of channel dopants. The curve is Poisson distribution.

seen in Fig. 2, the long-range part of the charge density varies smoothly and does not diverge at the origin.

To convert the discrete random dopants into the continuous doping profile for further 3D device simulation, we utilize the charge density derived from the long-range part of the ionized coulomb potential for each dopant [7]

$$\rho(r) = \frac{k_c^3}{2\pi^2} \frac{\sin(k_c r) - k_c r \cos(k_c r)}{(k_c r)^3}, \quad (2)$$

where  $r$  is the distance to the ionized dopant and  $kc$  is the reciprocal of screening length. To keep the total discrete dopants conserved, the doping concentration in (2) must be normalized within the device volume as:

$$\rho'(r) = \frac{\rho(r)}{\iiint_V \rho(r) dv} = \frac{\rho(r)}{\iiint_V \rho(r) r^2 \sin \theta dr d\theta d\phi}, \quad (3)$$

where  $V$  is the device volume.

#### IV. SIMULATION RESULTS

Based on an optimized transistor design template, for both HK/MG and Poly/SiON cases we studied 200 samples to investigate the RDF effects on the threshold voltage fluctuation and  $I_d$ - $V_g$  curves. Here we use a HKMG nMOSFET as an example. The final doping concentration is the summation of (3) for each dopant and is shown as Fig. 3. 200 samples are generated by MC method and followed by Sentaurus Device (SDevice) 3D simulation. The placement of each discrete dopant is randomly located in each mesh cell and the numbers of discrete dopants in each mesh cell must follow the Poisson statistics whose mean value is calculated from continuous doping concentration within the cell. This approach is employed to model the physical process of ion implant and diffusion behaviors, which results in random characteristics of discrete dopants. Therefore, Fig. 4 illustrates the distribution of the number of channel dopants followed a Poisson distribution. Fig. 5 shows the  $I_d$ - $V_g$  curves of the 200 statistical samples

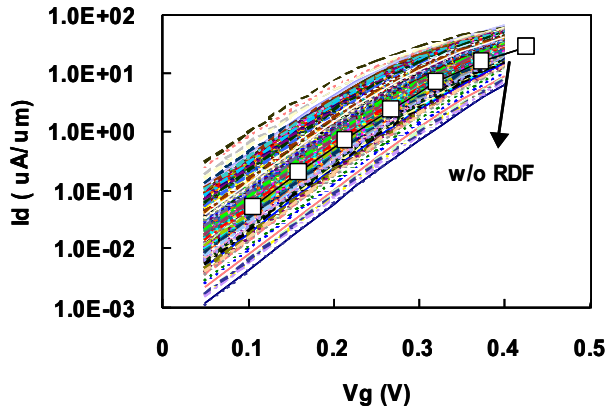


Figure 5. Id-Vg curves of RDF samples. The one without RDF is also shown for comparison.

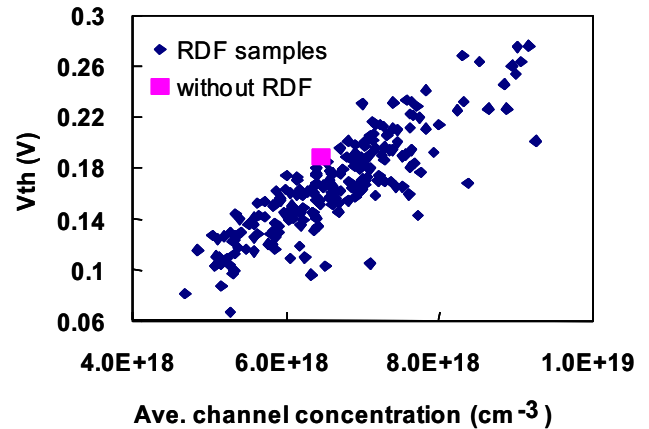


Figure 7. Vth v.s. the average channel concentration

and also the non-statistical one. The median  $V_{th}$  of the statistical samples is slightly smaller than the non-statistical one. This effect arises from the discrete nature of the dopant atoms causing an inhomogeneous channel potential [9]. Scatter plot of the  $V_{th}$  vs number of channel dopants for the statistical sample of 200 devices is shown in Fig. 6. As the number of channel dopant increases, the corresponding channel concentration increases which results in an increase of threshold voltage. Fig. 7 shows the  $V_{th}$  versus the average channel concentration and the point without RDF is also shown for comparison. The average channel concentration of RDF samples being distributed around the one without RDF shows the consistency and validity of our RDF simulation scheme.

### V. VARIABILITY OPTIMIZATION

Fig. 8 shows the prediction of  $\sigma V_{th}(RDF)$  ( $\sigma V_{th}$  due to RDF only) for SiON-Poly and HKMG nMOSFETs with the same  $I_{off}$ . The WFS of HKMG nMOSFET here is assumed to be 0.1V with respect to Si conduction band edge. Since HKMG device characteristics can be modulated by WFS, Fig. 9 shows the variability in terms of normalized RDF and CDU variations

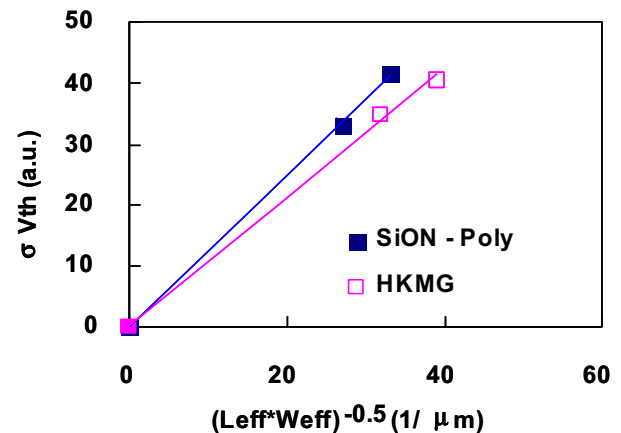


Figure 8. Pelgrom plot of SiON-Poly and HKMG nMOSFETs. The WFS of HKMG nMOSFET is 0.1V and EOT ratio between HKMG and SiON-Poly is about 0.7. The gate dielectric in either case is assumed to be ideal.

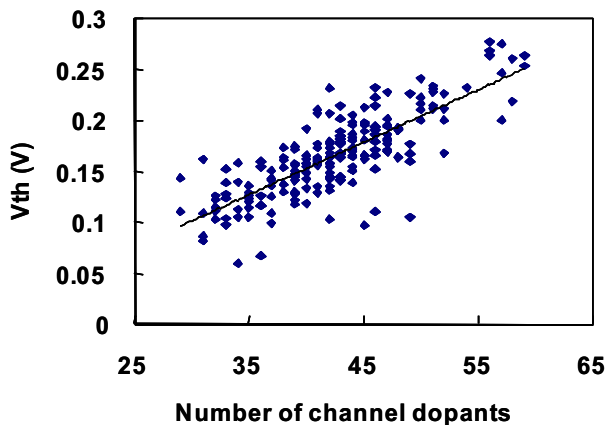


Figure 6. Vth v.s. the number of channel dopants.

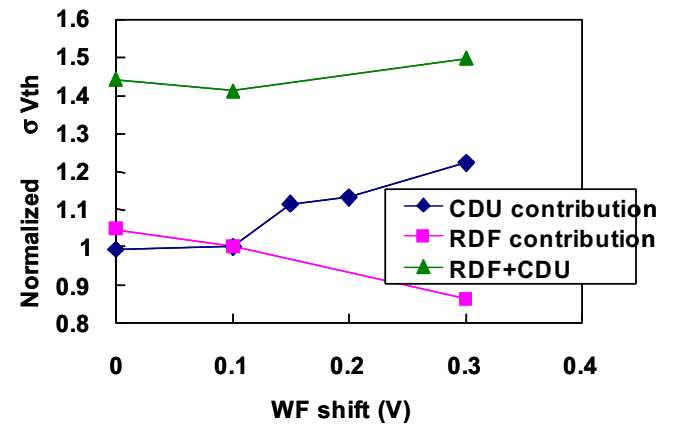


Figure 9. The normalized  $\delta V_{th}$  (RDF, CDU and their total effect) v.s. WFS. A minimum  $\delta V_{th}$  exists with optimum WFS.

versus WFS under a constant Ioff. For  $\sigma V_{th}(RDF)$ , as WFS increases, pocket dose reduces resulting in a decrease of  $\sigma V_{th}(RDF)$ . However, for  $\sigma V_{th}(CDU)$ , as WFS increases, less pocket dose leading to an increase of LDD encroachment causes an increasing CDU variation. Thus, there is a minimum variability with optimum WFS.

## VI. CONCLUSION

We present a 3D atomistic RDF in-house simulator which can model  $V_{th}$  fluctuations induced by discrete dopants in the non-uniform channel. A novel dopant discretization scheme using Poisson statistics that can achieve self-consistent median parametric values (e.g. average channel concentration) with deterministic device simulations was introduced. This capability was deployed to study the variability contributed from RDF and CDU under different WFS in advanced transistor structures with non-uniform channels. It is concluded that WFS can be employed to minimize the total variability.

## ACKNOWLEDGMENT

The authors are grateful to Dr. C. H. Diaz for his helpful comments and discussion

## REFERENCES

- [1] G. Tsutsui, K. Tsunoda, N. Kariya, Y. Akiyama, T. Abe, S. Maruyama, T. Fukase, M. Suzuki, Y. Yamagata, and K. Imai, "Reduction of  $V_{th}$  variation by work function optimization for 45-nm node DRAM cell" Symp. VLSI Tech., 2008
- [2] K. J. Kuhn, "Reducing variation in advanced logic technology: approaches to process and design for manufacturability of nanoscale CMOS," IEDM Tech, Digest, 2007.
- [3] A. Asenov, "Random dopant induced threshold voltage lowering and fluctuations in sub-0.1 $\mu$ m MOSFET's: a 3D atomic simulations study," IEEE Trans. Elec. Dev., Dec. pp. 2505-2513, 1988.
- [4] F-L Yang, J-R Hwang, H-M Chen, J-J Shen, S-M Yu, Y. Li, and D. D. Tang, "Discrete dopant fluctuated 20nm/15nm-gate planar CMOS," Symp. VLSI Tech., 2007.
- [5] C.H. Diaz et al., IEDM, Tech, Digest, 2008
- [6] K. F. Breena, The physics of semiconductors with applications to optoelectronic devices, Cambridge university press, 1999.
- [7] N. Sano, K. Matsuzawa, M. Mukai, and N. Nakayama, "Role of long-range and short-range coulomb potentials in threshold characteristics under discrete dopants in sub-0.1 $\mu$ m Si-MOSFETs," IEDM, Tech, Digest, 2000
- [8] A. Haug, Theoretical solid state physics, vol. 1, pergmon, New York, 1972
- [9] H-S Wong, and Y. Taur, "Three-dimensional atomistic simulation of discrete random dopant distribution effects in sub-0.1 $\mu$ m MOSFET's," IEDM, Tech, Digest, 1993